

Cite this: DOI: 10.1039/c1lc20213h

www.rsc.org/loc

PAPER

## Microfabricated polyester conical microwells for cell culture applications†

Šeila Selimović,<sup>‡,ab</sup> Francesco Piraino,<sup>‡,abc</sup> Hojae Bae,<sup>ab</sup> Marco Rasponi,<sup>c</sup> Alberto Redaelli<sup>c</sup> and Ali Khademhosseini<sup>\*abd</sup>

Received 9th March 2011, Accepted 21st April 2011

DOI: 10.1039/c1lc20213h

Over the past few years there has been a great deal of interest in reducing experimental systems to a lab-on-a-chip scale. There has been particular interest in conducting high-throughput screening studies using microscale devices, for example in stem cell research. Microwells have emerged as the structure of choice for such tests. Most manufacturing approaches for microwell fabrication are based on photolithography, soft lithography, and etching. However, some of these approaches require extensive equipment, lengthy fabrication process, and modifications to the existing microwell patterns are costly. Here we show a convenient, fast, and low-cost method for fabricating microwells for cell culture applications by laser ablation of a polyester film coated with silicone glue. Microwell diameter was controlled by adjusting the laser power and speed, and the well depth by stacking several layers of film. By using this setup, a device containing hundreds of microwells can be fabricated in a few minutes to analyze cell behavior. Murine embryonic stem cells and human hepatoblastoma cells were seeded in polyester microwells of different sizes and showed that after 9 days in culture cell aggregates were formed without a noticeable deleterious effect of the polyester film and glue. These results show that the polyester microwell platform may be useful for cell culture applications. The ease of fabrication adds to the appeal of this device as minimal technological skill and equipment is required.

### Introduction

Many research disciplines, such as biology, chemistry, physics, and different engineering fields, have seen a steady effort in reducing experimental systems from a macro- or benchtop to a micro- or lab-on-a-chip scale.<sup>1,2</sup> In particular, microscale platforms, such as microwells, have been used for cell analysis, culture and directed growth of cells.

Microwells have emerged as robust alternatives to traditional 2D cell culture substrates as they are relatively simple, and compatible with existing laboratory techniques and instrumentation. Another key reason for the use of such structures is the possibility of forming controlled-size cell aggregates.<sup>3,4</sup> A variety of platforms for fabricating microwells have been developed in

the past few years. For example, microwells can be integrated into poly(methyl methacrylate) (PMMA) plates,<sup>5</sup> fabricated from polymers such as poly(dimethylsiloxane) (PDMS) that are molded onto a substrate patterned with photoresist,<sup>6–9</sup> formed from hydrogels such as poly(ethylene glycol) (PEG) that are molded onto a polymer master,<sup>10</sup> or from hydrogels that are selectively photocrosslinked through a transparency mask.<sup>11</sup> Any changes in the design of PDMS or hydrogel platforms require printing of a new mask and photolithography fabrication of a new silicon master, which raises the cost and time of the process. Microwells can also be fabricated from PDMS using the laser sintering process,<sup>12</sup> in which thin layers of the polymer are deposited in the desired shape, or can be etched into glass.<sup>13</sup> The use of parylene-C,<sup>14</sup> paper spotting,<sup>15</sup> and surface functionalization<sup>16</sup> has also been investigated, but these methods are not widely used for microwell fabrication.

In contrast to photolithographic techniques, automatic laser micromachining is an alternative method<sup>17–19</sup> for fabricating microwells. Laser micromachining involves ablation of a material, that is, removal of matter in the form of clusters or smaller constituents, e.g. molecules and ions, via short bursts of monochromatic light.<sup>18</sup> Depending on the type of laser used and thus the amount of energy delivered to the matter, a strongly absorbing material, for example certain polymeric films such as polyester, may experience bond breakage and vaporization (e.g. with UV or excimer lasers). Alternatively, multiphoton

<sup>a</sup>Center for Biomedical Engineering, Department of Medicine, Brigham and Women's Hospital, Harvard Medical School, Cambridge, Massachusetts, 02139, USA

<sup>b</sup>Harvard-MIT Division of Health Sciences and Technology, Massachusetts Institute of Technology, Cambridge, Massachusetts, 02139, USA

<sup>c</sup>Bioengineering Department, Politecnico di Milano, Piazza Leonardo da Vinci 32, 20133 Milan, Italy

<sup>d</sup>Wyss Institute for Biologically Inspired Engineering, Harvard University, Boston, Massachusetts, 02115, USA. E-mail: alik@rics.bwh.harvard.edu

† Electronic supplementary information (ESI) available. See DOI: 10.1039/c1lc20213h

‡ These authors contributed equally to this article.

absorption can lead to thermal depolymerization and melting, which has been observed with weak lasers, such as CO<sub>2</sub> lasers.<sup>18</sup> Melting of the material leads to the formation of conical features, which is an intrinsic characteristic of this type of material processing and contrasts with other techniques such as mechanical drilling.<sup>17</sup> Polyester films in research have mainly been used for manufacturing 3D devices consisting of channels, mixers and reservoirs<sup>20,21</sup> on several connected layers, *via* laser micromachining. We are not, however, aware of published work that investigates the use of polyester films in microwell fabrication or for other biological applications, even though this material promises a cheap and simple device fabrication, especially when subjected to a direct write method.<sup>22</sup>

In this work, we developed a fast and low-cost method to form cell aggregates, using polyester film as a microfabricated platform containing conical microwells. Individual polyester sheets pre-coated with silicone adhesive on both sides were stacked together to achieve the desired thickness, which later was used to determine the microwell depth. Then, the microwells were cut into the stack by using a laser engraver. The thicker the stack, the less pronounced the conical shape of the features. Microwells fabricated by engraving polyester films could easily be combined with microfluidic channels that are manufactured in the same fashion. Then they could be sealed with a second glass slide or a PDMS slab, thereby forming a self-contained, insulated device. This technique is attractive due to reproducibility and lends itself to automated manufacturing. Additionally, the depth of the wells could be adjusted by stacking individual polyester layers together. Thus, fabricating a 350  $\mu\text{m}$  thick device was as simple and fast as fabricating a 50  $\mu\text{m}$  device. In contrast, any changes in the design of PDMS or hydrogel platforms require printing of a new mask and fabrication of a new silicon master, which increases the cost and time of fabrication. The stacking of several layers of polyester film is in particular a flexible solution, when only one type of film is available. Otherwise, a thicker film can be used to achieve the same effect. Last, stacking several layers of film has the advantage of printing high aspect ratio features. In this particular case, several polyester layers can be printed individually, for example at 1 : 1 aspect ratio, and then stacked to achieve a high aspect ratio feature. This is an additional advantage of laser printing of polyester film compared to standard PDMS replica, where only a single master wafer can be used and high aspect ratio features are limited by the structural integrity of both the master photoresist and the PDMS.

Since the polyester sheets are pre-coated with a silicone adhesive, the polyester platform could be bonded to glass, PDMS, or other polyester substrates, introducing yet another level of flexibility. We manufactured devices with different well diameters and depths and demonstrated their practical use in cell aggregate studies. We compared our results for murine embryonic stem cells (ES cells) and human hepatoblastomas in terms of cell adhesion and cell aggregate growth to PEG and PDMS microwell platforms. In addition, the capability of realized microwells to release cell aggregates upon formation and culture was assessed and measured, yielding release efficiency coefficients (fraction of successfully released cell aggregates). We demonstrate that this fabrication method is simple, cheap and reliable for cell cultures in which aggregate formation is required.

## Materials and methods

### Polyester film

The polyester film (product number NT 8512-2DL, Adhesive Applications) is 50.8  $\mu\text{m}$  thick, and is supplied with 38.1  $\mu\text{m}$  thick silicone adhesive on both sides, ready for use. The adhesive is protected with a polyester release liner, 50.8  $\mu\text{m}$  in thickness. The film is designed to resist temperatures from  $-51\text{ }^{\circ}\text{C}$  to  $177\text{ }^{\circ}\text{C}$  and is thus suitable for laser engraving.

### Device fabrication

Well arrays were fabricated according to the steps outlined in Fig. 1a. A digitized microfluidic layout created in CorelDraw software was transferred onto the polyester film by thermal ablation from a computer-controlled CO<sub>2</sub> laser machine (VLS2.30,  $\lambda = 10.6\text{ }\mu\text{m}$ , VersaLASER). The maximum laser power provided by the laser engraver was 30 W, and the maximum write speed was  $114.3\text{ cm s}^{-1}$ . Microwells of two diameter sizes (150 and 300  $\mu\text{m}$ ) were cut into polyester sheets, with an aspect ratio approaching 1 : 1.

We generated single-layer devices (referred to as “150  $\mu\text{m}$  chip”) that consisted of a single sheet of polyester with a well diameter of 150  $\mu\text{m}$  and a thickness of 178  $\mu\text{m}$ , which included two layers of silicone adhesive and a release liner on the upper side. We also generated double-layer devices (referred to as “300  $\mu\text{m}$  chip”) that consisted of two sheets of polyester with a well diameter of 300  $\mu\text{m}$  and a final thickness of 305  $\mu\text{m}$ . As the wells had a conical shape, these dimensions describe the bottom opening of the wells. Both devices contained an array of 100 wells and the well volume was on the order of a few nL. The x-directional spacing of the wells was 1 mm, and the y-directional

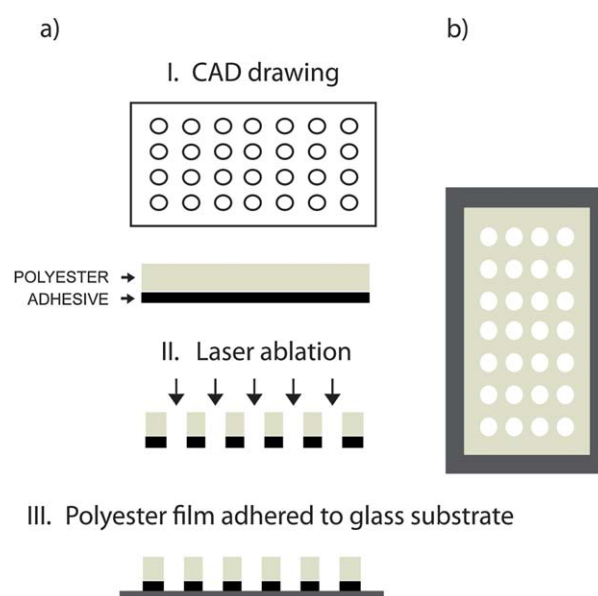


**Fig. 1** Schematic of the polyester microwell device fabrication process. (a) Fabrication steps: a drawing is generated in a CAD program (I) and used as a pattern for laser ablation of the polyester film (II). Finally, the patterned film is adhered onto a glass substrate through an adhesive side (III). (b) Top view of the device.

spacing was 2 mm. Each device was glued onto a separate, untreated 1 mm thick glass slide, such that the wells were closed on one side and open on the other side.

To determine the optimal laser engraving conditions to produce wells with diameters of 150  $\mu\text{m}$  and 300  $\mu\text{m}$ , an array of wells with drawn diameters between 50  $\mu\text{m}$  and 500  $\mu\text{m}$  was printed on both single- and double-layer devices. For this purpose laser powers and write speeds ranging from 3 to 10 W and from 11.4 to 57  $\text{cm s}^{-1}$  were tested, respectively. The resulting round wells were characterized in terms of the average diameters of their bottom surfaces, by analyzing optical microscopy images (Nikon Eclipse Ti, 20 $\times$  objective) using ImageJ software.

We studied in the same fashion the effect of engraving conditions on the eccentricity and printed an array of microwells with the ratio of semiminor to semimajor axis ranging from 1 : 1 to 1 : 3, on both a single-layer and double-layer device. Eccentricity is defined as

$$e = \sqrt{1 - (b^2/a^2)},$$

where  $a$  is the semimajor axis and  $b$  is the semiminor axis. We measured  $a$  and  $b$  for all wells and found the average eccentricity of printed features as a function of the eccentricity of the drawn features.

### Scanning electron microscopy (SEM)

Microwells on the 150  $\mu\text{m}$  and 300  $\mu\text{m}$  chips were imaged using a FESEM Ultra 55 scanning electron microscope (Zeiss, Germany). Samples were mounted onto aluminium stages, sputter-coated with gold for 90 s and imaged at a working distance of 26 mm under an accelerating voltage of 5 kV.

### Murine ES cell culture and aggregate formation

All tissue culture components were purchased from Gibco-Invitrogen Corporation unless otherwise indicated. The R1 ES cells line was cultured in high glucose-Dulbecco's Modified Eagles Medium (DMEM) supplemented with 10% (v/v) ES qualified FBS, 100 U  $\text{ml}^{-1}$  penicillin and 100  $\mu\text{g ml}^{-1}$  streptomycin, 1% (v/v) nonessential amino acid solution, 1 mM L-glutamine, 0.1 mM  $\beta$ -mercaptoethanol, and 1.00 U  $\text{ml}^{-1}$  of leukemia inhibitory factor (LIF, Millipore). ES cells were kept undifferentiated by changing media daily and were passaged every 2 days with a subculture ratio of 1 : 4. All microwell devices were placed in 4 well culture plates after fabrication, washed with ethanol for 2 hours, and kept in PBS overnight, until cell seeding, in an incubator.

To seed an array of 100 microwells, 2 ml of a solution containing  $1 \times 10^6$  cells per ml was placed on top of the array and kept at ambient temperature for 15 min to allow for cell sedimentation on the array surface. Subsequently, microwell arrays were gently washed with PBS to remove cells on the polyester surface and immersed in fresh culture medium. Aggregates within wells were cultured in alpha Minimal Essential Medium ( $\alpha$ -MEM) containing 15% FBS and 1% penicillin/streptomycin. We exchanged the medium daily over a period of 9 days. Cells were maintained in a humidified incubator at 37  $^\circ\text{C}$  with a 5%  $\text{CO}_2$  atmosphere. For aggregate formation, LIF was omitted from the medium. Daily monitoring of cell conditions was

established through optical inspection with an inverted phase-contrast microscope (Nikon Eclipse Ti, 10 $\times$ ). At the same time images of individual wells were acquired to evaluate changes in cell aggregate formation and growth.

### HepG2 cell culture and aggregate formation

Human hepatoblastoma cells (HepG2 cells) were cultured at 37  $^\circ\text{C}$  in a 5%  $\text{CO}_2$  humidified incubator in culture medium containing 89% DMEM, 10% FBS, and 1% penicillin-streptomycin. All microwell devices were placed in 4 well culture plates after fabrication, washed with ethanol for 2 hours, and kept in PBS overnight, until cell seeding, in an incubator. HepG2 cells were trypsinized and seeded in microwells in a similar manner as the ES cells. Subsequently, microwell arrays were gently washed with PBS to remove cells on the polyester surface and immersed in fresh culture medium. Seeded microwell arrays were kept in a 5%  $\text{CO}_2$  humidified incubator at 37  $^\circ\text{C}$  for 9 days. Microscope images were taken daily to analyze aggregate formation in microwells, as explained above.

### Protein adsorption

Texas-red (TR) conjugated bovine serum albumin (BSA) was dissolved in PBS solution (pH  $\approx$  7.4) at 50  $\mu\text{g ml}^{-1}$ . To test protein adsorption on polyester films, specifically the polyester release liner, 50  $\mu\text{l}$  of the protein solution was evenly distributed on the surfaces and incubated for 20 minutes at room temperature in a dark environment. After incubation samples were washed twice with PBS and analyzed under a fluorescent microscope (Nikon Eclipse Ti). Fluorescence images were analyzed using ImageJ software (<http://rsbweb.nih.gov/ij/>). Pixel intensities were averaged for 3 image fields for each of the three independent experiments. Intensities were normalized to a glass control and also compared to polystyrene (product number 351147, Becton Dickinson Labware).

### Cell adhesion

For 2D cell adhesion studies, cells were trypsinized and seeded at a concentration of 166 cells per  $\text{mm}^2$  onto the polyester release liner, untreated glass slides (Fisher) and tissue culture treated polystyrene (product number 353047, Becton Dickinson Labware). After incubation at 37  $^\circ\text{C}$  for 4 h, the three substrates were dipped into PBS to remove non-adherent cells. Three random images were taken from each surface and adherent cells were counted. Results were normalized to the glass control and all experiments were performed in triplicate. The same procedure was followed independently for both ES and HepG2 cells.

### Cell aggregate formation and growth measurement

Four independent experiments were conducted, namely ES and HepG2 cells culture in both 150  $\mu\text{m}$  and 300  $\mu\text{m}$  wells. All experiments were conducted in triplicate. All wells were imaged before and immediately after cell seeding, as well as on days 3 to 9. We recorded the number and measured the diameters of HepG2 and ES cell aggregates growing in each well.

We used the ImageJ Area function to measure the area of each cell aggregate large enough to be observed under a 10 $\times$  objective;

the minimum area resolution was 20  $\mu\text{m}$ . When wells contained more than one cell aggregate in the early stage of culture, we added the areas of all cell aggregates in a well and calculated the corresponding aggregate diameter, assuming that all aggregates had a circular cross-section. We then averaged across 300 wells on three separate devices.

### Cell viability and aggregate retrieval efficiencies

A calcein-AM/ethidium homodimer Live/Dead assay (Invitrogen) was used to quantify cell viability within the microwells according to the manufacturer's instructions. After the 9-day cell culture, the medium was aspirated; the devices were transferred to new polystyrene dishes and washed with PBS. We then incubated the formed cell aggregates in 50  $\mu\text{l}$  of 4 mM ethidium homodimer (EthD) and 2 mM calcein-AM in PBS at 37  $^{\circ}\text{C}$ . After 10 minutes we washed the devices again with PBS and imaged the cells. Live cells stained green due to the enzymatic conversion of the non-fluorescent cell-permeant calcein-AM to fluorescent calcein. Dead cells stained red after binding of EthD to the DNA of membrane-compromised cells.

After the cell viability analysis, on day 9 of cell culture, the devices were gently tilted and washed with 1 ml PBS in order to remove the formed cell aggregates from the microwells. We counted the number of retrieved aggregates and normalized it against the number of all cell aggregates.

### Statistical analysis

Statistical analysis was performed using the 2-way ANOVA test for the protein adsorption and cell adhesion measurements, with  $p < 0.05$  considered as statistically significant.

## Results and discussion

### Microwell fabrication

To determine the optimal laser engraving conditions to achieve the two desired well diameters, an array of wells with drawn diameters between 50  $\mu\text{m}$  and 500  $\mu\text{m}$  was printed on both a single-layer and double-layer device by varying the laser power and write speed. The following settings resulted in uniform wells of the desired sizes. For a 150  $\mu\text{m}$  well, we began with a drawing of a 100  $\mu\text{m}$  well, and then used the laser at 3 W and a write speed of 17.1  $\text{cm s}^{-1}$ . For a 300  $\mu\text{m}$  well, we drew a 200  $\mu\text{m}$  well, then used the laser at 7.5 W and a write speed of 11.4  $\text{cm s}^{-1}$  (Fig. 2). The standard deviation in well diameter from 100 wells was 4.2% for the 150  $\mu\text{m}$  chip and 1.8% for the 300  $\mu\text{m}$  chip, indicating high feature fidelity. Table S1 (ESI $\dagger$ ) lists the different printing parameters and resulting well sizes.

SEM images of the fabricated wells can be seen in Fig. 3a–d. The minimum reliably achievable pitch in the well array (center-to-center distance) was 750  $\mu\text{m}$ . This limit was due to the melting of the top surface of the film and the subsequent formation of tall rings around the well perimeters.

We observed two important trends among the data presented in Table S1 $\dagger$ : increasing the power yielded larger features and increasing the write speed yielded smaller and less uniform features. Namely, the more energy was delivered to a particular location on the film, the more melting occurred, and thus the

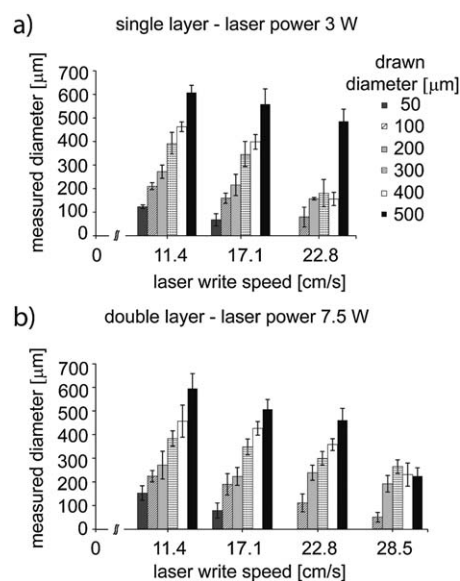


Fig. 2 Selected printing parameters (laser power, laser write speed and drawn diameter) and the corresponding measured microwell diameters.

printed feature became larger. We observed the effect of the laser power on the final feature size to be slightly more pronounced (Table S1 $\dagger$ ) than the effect of the laser write speed. In few cases the measured microwell size was smaller than expected; this was due to incomplete melting of the polyester film, which left a hard residue inside the well.

We also observed that the features drawn as perfect circles (eccentricity  $e = 0$ ) resulted in microwells with a non-zero eccentricity, regardless of laser power and write speed. In turn, features drawn as ellipses with a particular non-zero eccentricity became more circular microwells using the same printing parameters. This artifact was a consequence of the mechanical limitations of the belt-driven laser beam actuator, which introduced a systematic feature elongation along the main laser plotting axis, and resulted in elliptical holes with the semimajor axes pointing in the same direction.

The measured diameters listed in Table S1 $\dagger$  were averages of minor and major axes for a measured eccentricity of 0.67. In Fig. 3e we show the relationship between the eccentricity of drawn features and the resulting microwells, at the ideal printing parameters for the two chosen well sizes. Our data indicate that if needed, relatively circular features could be achieved when the features were drawn as ellipses with semimajor to semiminor axis ratios of 3 : 1 (for 150  $\mu\text{m}$  wells) and 1.2 : 1 (for 300  $\mu\text{m}$  wells).

The conical well profile (Fig. 3f) was recorded with a stylus profilometer (12.5  $\mu\text{m}$  tip radius, Sloan Technology Corp. Dektak IIA). This feature shape is largely due to the melting of the various layers of the device and the accumulation of ablated material on the well perimeter. Namely, the deeper the laser penetrates into the material, the more material is expelled and migrates outward, resulting in a larger opening on the top than on the bottom surface of the device.<sup>17</sup> The printing parameters were chosen such that the well bottom had the desired diameter, and the well opening was on average 400  $\mu\text{m}$  wide for the 150  $\mu\text{m}$  wells and 550  $\mu\text{m}$  for the 300  $\mu\text{m}$  wells. We also tested the effect of a wide range of laser powers and write speeds on the taper

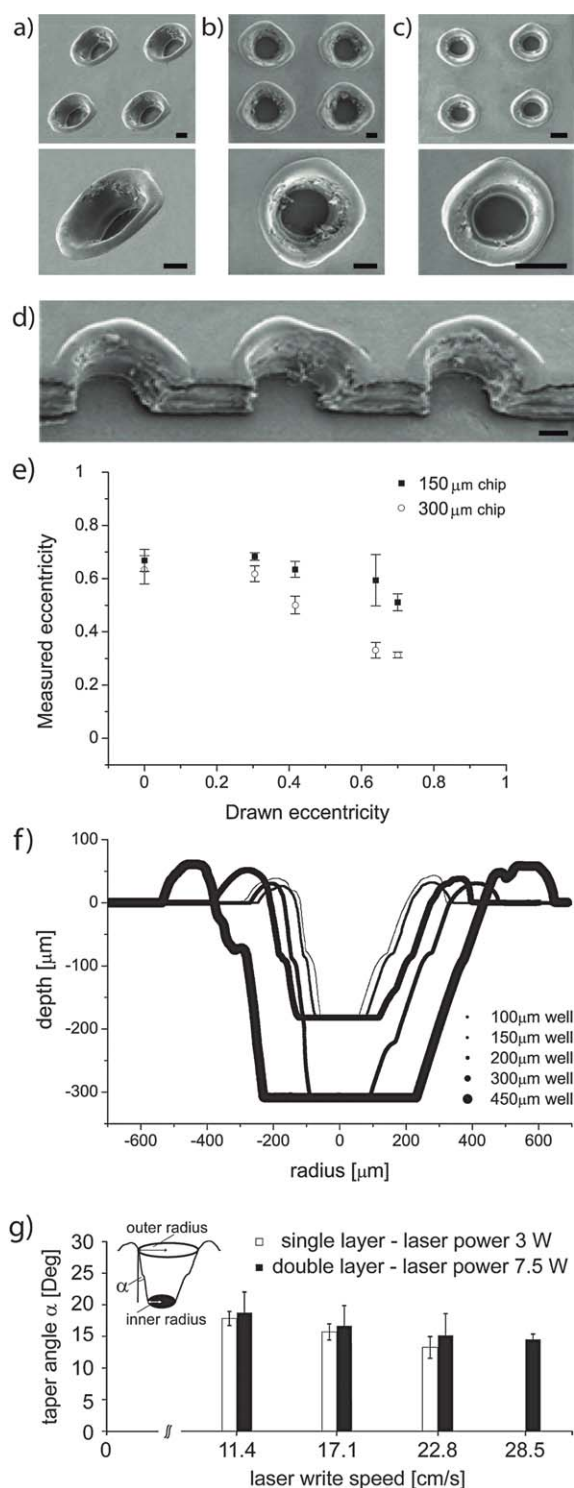


**Fig. 3** SEM images of a double layer polyester device with a height of 300  $\mu\text{m}$  in (a) oblique view and in (b) top view and of a single layer polyester device with a height of 178  $\mu\text{m}$  in top view (c), at 100 $\times$  and 500 $\times$  magnification. (d) SEM profile of double layer deep wells. (e) Relationship between designed and measured eccentricity of round features, when engraved into polyester sheets. (f) Profilometer measurements of a range of well designs, indicating the conical well profile. (g) Schematic representation of taper effects by laser ablation onto single and double polyester layers ( $\alpha$  is the taper angle) and plot of taper angle vs. laser write speed. All scale bars are 150  $\mu\text{m}$ .

angle (Fig. 3g) of the conical wells. Our observations indicate that an increase in cumulative energy delivered to the device (high power and low write speed) resulted in larger taper angles and thus in a more pronounced conical shape of the holes. This observation is in agreement with our general understanding of the formation of the taper, but a more detailed study that would elucidate the underlying physical processes is outside of the scope of this work. Choosing to retain the taper angle intrinsic to the optimal printing parameters had the added benefit that the manufacturing process had few steps. If cylindrical wells or wells with different taper angles were desired, the patterned features could be exposed again to the laser at a different power setting, or the same features could be printed again from the reverse side, thus requiring an additional manufacturing step and alignment of the patterned features with the laser. We note that deep wells with more uniform profiles could be fabricated from thicker polyester films, however, if these are not available to the experimenter, stacking several film layers can be used as a substitute.

It has been shown that the shape of the microwells affects the circulation of medium inside the wells, which in turn influences cell growth.<sup>23</sup> For example, when growth medium is changed or added to a cell culture, conical or concave wells allow for better fluid circulation around the growing cell aggregate bodies than cylindrical wells.<sup>23,24</sup> Further, these studies showed that the velocity and shear stress distribution is more uniform in concave and conical wells compared to cylindrical wells, enabling more uniform cell seeding. Thus, the availability of conical microwells on this platform is advantageous for cell culture.

During the printing process, the polyester film absorbed laser energy, such that the material adjacent to the laser beam melted, an effect that was also observed in harder materials, such as glass.<sup>18</sup> As a result, a 40–50  $\mu\text{m}$  tall and 100  $\mu\text{m}$  wide ring of melted film formed around the edge of each microwell (Fig. 3a–d). We did not polish the device and remove these rings, as our goal was to keep the device fabrication simple. Moreover, the presence of a tall ring around the edge of a microwell could be exploited to conveniently increase the well depth, if so desired. A potential drawback of this occurs when the microwell platform is to be bonded with an additional layer of microfluidic channels printed in polyester film. In this case the rough surface of the microwell layer could lead to air bubbles being trapped and leaking of fluid between the wells and the channels. A simple solution in this case is to remove the melted, rough top liner of the microwell platform. The surface underneath is even and coated with adhesive and it can be glued to additional polyester layers. Alternatively, the ring can be removed by gently moving a razorblade across the device surface.

### Protein adsorption and cell adhesion on polyester surfaces

To determine the utility of the polyester films for cell culture, we evaluated the resistance of polyester to protein adsorption and to ES cell and HepG2 cell adhesion (Fig. 4). Protein adsorption on polyester was shown to be significantly lower than on glass or polystyrene, namely only 10% of the adsorption value on glass (Fig. 4b).

### Cell aggregate formation and growth

Some cell types such as hepatocytes and ES cells benefit from being cultured on 3D platforms instead of planar surfaces.<sup>25</sup>

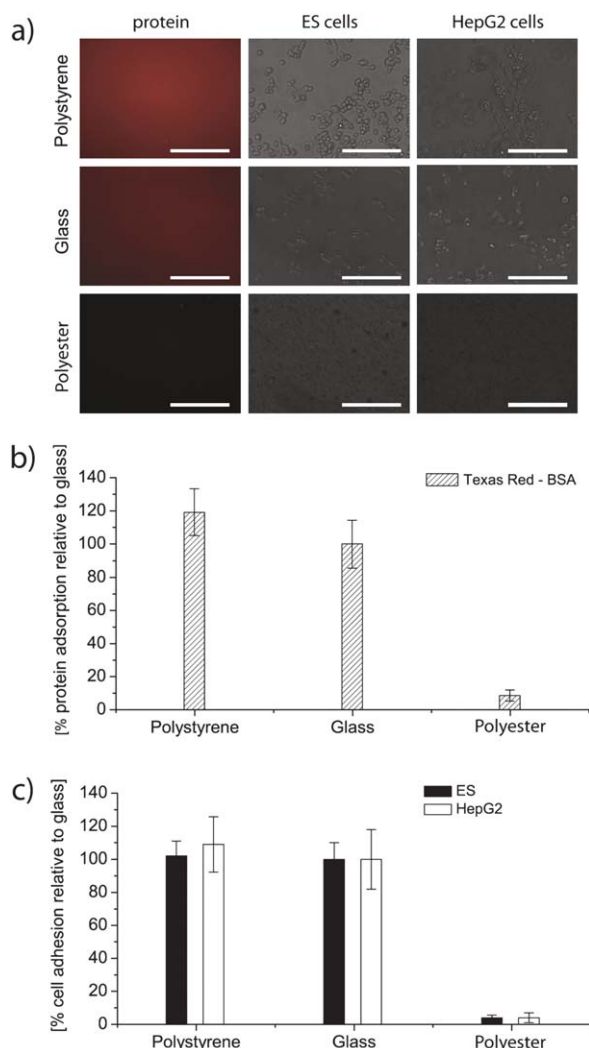


**Fig. 4** Cell adhesion after 4 hours of incubation and protein adsorption after 20 min of incubation on polyester film. (a) Fluorescence and phase images of protein and cell coated polystyrene, polystyrene and glass. Scale bars are 150  $\mu\text{m}$ . (b) Protein adsorption and (c) cell adhesion expressed in percentages relative to adhesion and adsorption on untreated glass and compared to polystyrene. The error bars are the standard deviation across three independent experiments. The differences between cell and protein adhesion values on polyester and glass and between polyester and polystyrene are statistically significant, as  $p < 0.05$  in all cases.

Particularly, the initial size of ES cell aggregates is one of the critical factors that control cell differentiation.<sup>26</sup> The resulting cell aggregates are referred to as “spheroids” for hepatocytes or “embryoid bodies” for ES cells, although for simplicity we use the term “aggregates” in this paper. In 3D culture these cell aggregates are known to maintain their metabolism and growth activity, and differentiate.<sup>27,28</sup> Using this platform for growing cell aggregates we made two main observations: (1) the cell culture on our polyester microwell chip resulted in the formation of cell aggregates and (2) the aggregate dimension was controlled by the size of the microwell structure. Both observations are consistent with published results on other array platforms, such as PEG<sup>29</sup> and PDMS<sup>10</sup> microwells.

Cells seeded on the device were trapped in each microwell and accumulated in the well within one day of culture. Cell aggregates

formed within three days on all devices and retained their shape for the duration of culture (9 days). Previously published studies<sup>23,24</sup> indicate that a conical well shape benefits both uniform cell seeding and formation of a single cell aggregate per well, as this shape is similar to the rounded shape of the aggregate, and the shear stress and flow velocity profile inside wells are more uniform than in cylindrical wells.

In 3D constructs such as our polyester microwell array, oxygen and nutrients necessary for cell survival were supplied *via* diffusion through the medium from the well opening to the well bottom, and during exchange of medium *via* convection. The convection driven material supply has been shown to be more efficient in conical than in cylindrical structures.<sup>23</sup> Thus, the efficiency with which the spherical constructs take up oxygen and nutrients may regulate the diameter of derived cell aggregates.

Typical phase contrast images of both cell types and on both devices are shown in Fig. 5a and b, for culture days 3, 6 and 9. The average cell aggregate size for days 3 to 9 is reported in Fig. 5c. We could not distinguish cell aggregates prior to day 3, as we did not pack the wells fully with cells during the seeding process. We expect that filling each well completely would result in observable cell aggregates earlier in the cell culture period.

By day 9 most cell aggregates were as large as the microwell. The average aggregate size on day 9 was 141  $\mu\text{m}$  and 290  $\mu\text{m}$  for the ES cells in 150  $\mu\text{m}$  and 300  $\mu\text{m}$  wells, respectively. For HepG2 cells, the average sizes were 141  $\mu\text{m}$  and 276  $\mu\text{m}$  for the two well sizes. The largest standard deviation for a single polyester device was 21  $\mu\text{m}$  and 16  $\mu\text{m}$  for ES cells, and 13  $\mu\text{m}$  and 11  $\mu\text{m}$  for HepG2 cells, but the average diameter varied only within 10  $\mu\text{m}$  between three devices.

We hypothesize that the large standard deviation of aggregate sizes on a single chip stemmed from the fact that the wells were not fully packed. Additionally, some aggregates may have been washed away from the wells during the exchange of medium, which increased the standard deviation. Because the variation in average aggregate size was small across three different chips, however, we consider our experimental results of cell aggregate growth robust and repeatable.

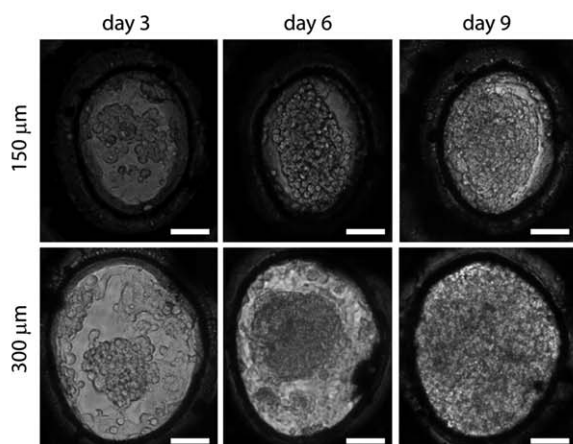
The exchange of medium and oxygen is more efficient in conical than in cylindrical wells,<sup>23</sup> which could have influenced the aggregate growth rate, especially in the early stages of culture. Regardless of platform, the aggregates reached the same average size by the end of culture both in our work and on the PEG and PDMS platforms.

We attribute the difference between the size of the aggregate and the size of the microwell to the observation that our wells were initially not fully packed with cells, thus our aggregates were smaller on day 3 than on other platforms. We also fabricated a polyester device with PDMS as the substrate to further improve the oxygen delivery to the microwells, but finally opted for a glass platform in these experiments, as glass is easier to use.

### Cell viability and aggregate retrieval

We imaged the fluorescently labeled cell aggregates before and after recovery from the polyester device. As it can be seen in Fig. 6 most of the aggregates were labeled green and only a small fraction of cells appeared red under the microscope (Fig. 6a). This observation indicates that all cell aggregates were viable

## a) HepG2 cells



## b) ES cells

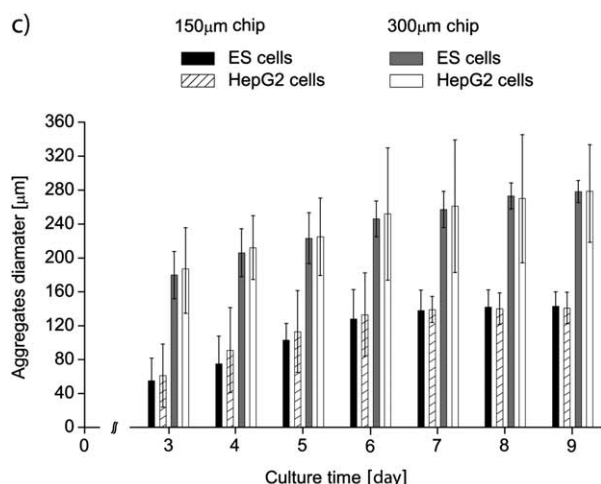
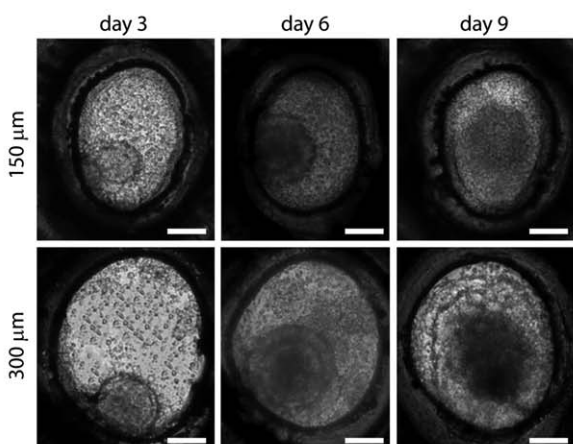


**Fig. 5** Representative images of aggregates formed by HepG2 (a) and ES cells (b) on days 3, 6 and 9 of cell culture and in the 150 and 300 μm wells. (c) Increase in the aggregate diameters of HepG2 and ES cells. All experiments were conducted in triplicate. The reported values are averages across 100 wells per device and three devices, and the error bars represent the standard deviation. All scale bars are 150 μm.

after a culture period of 9 days on the polyester platform and, further, that neither the polyester film nor the silicone adhesive had a deleterious effect on the cell viability.

After the viability assay, cell aggregates were retrieved from the microwells by gently tilting the devices and washing them with PBS (Fig. 6b and c). The number of retrieved aggregates from each sample was determined by counting using low magnification (2×) phase contrast images.

Aggregates remaining inside the polyester microwells after the washing step as well as broken aggregates were not counted. The percentage of released aggregates was found by comparing the total number of aggregates released from a single microwell array to the total number of occupied microwells on that array. The percentages of retrieved aggregates between different devices were also compared (Fig. 6d) and ranged from 57% for the 150 μm chip to 70–75% for the 300 μm chip.

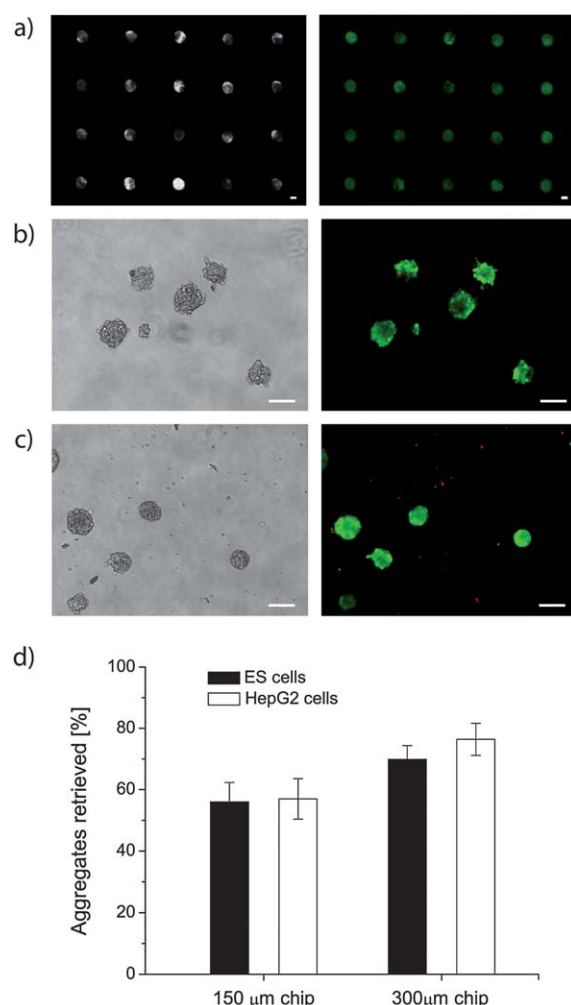


**Fig. 6** (a) Phase contrast and fluorescence images of ES cell-derived aggregates on day 9 of culture in 300 μm wells. Green fluorescence indicates live, red fluorescence indicates dead cells. (b) Typical retrieved cell aggregates in phase contrast and fluorescence images: ES cells aggregates and (c) HepG2 cells, both formed in 150 μm wells. Scale bars are 150 μm. (d) Retrieval rate of ES cell and HepG2 cell aggregates from 150 and 300 μm wells after a 9 day culture. The error bars are standard deviation, with  $n = 3$ .

Aggregates were more easily released from the larger wells. The cell type did not have an observable effect on the robustness of aggregates, as the retrieval efficiency was similar for ES and HepG2 cells. Our release efficiencies for the 150  $\mu\text{m}$  chip were lower than those for the PEG platform (80%).<sup>10</sup> We suspect that our cell aggregates adhered to the glass substrate, which lowered our retrieval efficiency.

Limitations of this technique are set by the width of the laser beam (50  $\mu\text{m}$ ) and by the thickness of a single polyester layer. However, it is possible to overcome some of these limitations by access to thinner films and advanced equipment, although the dimensions generated in this study are sufficient for cell culture applications.

In the future, we plan to develop a self-contained, independent and portable cell-culture platform, which includes both fluidic channels and microwells. We envision that the end product will be sufficiently simple to produce so that the fabrication can be automated and the device can be used in other academic research laboratories and the industrial environment.

## Conclusions

We fabricated arrays of conical microwells by laser ablation of an adhesive polyester film. The patterned film was then glued onto untreated glass slides. We showed that we could control the well depth, diameter and eccentricity by stacking layers of polyester and adjusting the printing parameters. The polyester microwells presented in this paper can be used to generate cell aggregates similar to other platforms. Advantages of this platform over others include convenience and the low cost of device fabrication, as well as the conical well profile, which enhances oxygen and medium delivery to the cell aggregates. Furthermore, our device can be fabricated with minimal microfabrication skill, and the direct writing method benefits from no tool tear and wear. Therefore, the presented polyester platform can be used as an alternative to standard PEG and PDMS devices for cell culture applications.

## Acknowledgements

This paper was supported by the National Institutes of Health (EB008392; DE019024; HL099073; AR057837; HL092836), National Science Foundation (DMR0847287), the Institute for Soldier Nanotechnology, the Office of Naval Research, and the US Army Corps of Engineers. F. Piraino was funded by a Progetto Rocca Visiting PhD Student Fellowship. We thank Adhesive Applications for providing us with polyester film samples, and Ben Wang and Halil Tekin for assistance with SEM.

## References

- 1 A. Khademhosseini, R. Langer, J. Borenstein and J. P. Vacanti, *Proc. Natl. Acad. Sci. U. S. A.*, 2006, **103**, 2480–2487.
- 2 G. M. Whitesides, *Nature*, 2006, **442**, 368–373.
- 3 M. Charnley, M. Textor, A. Khademhosseini and M. Lutolf, *Integr. Biol.*, 2009, **1**, 625–634.
- 4 J. M. Karp, J. Yeh, G. Eng, J. Fukuda, J. Blumling, K. Y. Suh, J. Cheng, A. Mahdavi, J. Borenstein, R. Langer and A. Khademhosseini, *Lab Chip*, 2007, **7**, 786–794.
- 5 R. Mori, Y. Sakai and K. Nakazawa, *J. Biosci. Bioeng.*, 2008, **106**, 237–242.
- 6 A. Khademhosseini, J. Yeh, G. Eng, J. Karp, H. Kaji, J. Borenstein, O. C. Farokhzad and R. Langer, *Lab Chip*, 2005, **5**, 1380–1386.
- 7 C.-H. Hsieh, C.-J. Huang and Y.-Y. Huang, *Biomed. Microdevices*, 2010, **12**, 897–905.
- 8 C.-H. Hsieh, J.-L. Wang and Y.-Y. Huang, *Acta Biomater.*, 2011, **7**, 315–324.
- 9 C. Han, Q. Zhang, R. Ma, L. Xie, T. Qiu, L. Wang, K. Michelson, J. Wang, G. Huang, J. Qiao and J. Cheng, *Lab Chip*, 2010, **10**, 2848–2854.
- 10 H.-C. Moeller, M. K. Mian, S. Shrivastava, B. G. Chung and A. Khademhosseini, *Biomaterials*, 2008, **29**, 752–763.
- 11 A. Revzin, R. G. Tompkins and M. Toner, *Langmuir*, 2003, **19**, 9855–9862.
- 12 E. Jung, D. Manassis, A. Neumann, L. Boettcher, T. Braun, J. Bauer, H. Reichl, B. Iafelice, F. Destro and R. Gambari, *Microsyst. Technol.*, 2008, **14**, 931–936.
- 13 H. Zhu, M. Holl, T. Ray, S. Bhushan and D. R. Meldrum, *J. Micromech. Microeng.*, 2009, **19**, 065013.
- 14 S. Jinno, H.-C. Moeller, C.-L. Chen, B. Rajalingam, B. G. Chung, M. R. Dokmeci and A. Khademhosseini, *J. Biomed. Mater. Res. A*, 2008, **86**, 278–288.
- 15 R. Derda, A. Laromaine, A. Mammoto, S. K. Y. Tang, T. Mammoto, D. E. Ingber and G. M. Whitesides, *Proc. Natl. Acad. Sci. U. S. A.*, 2009, **106**, 18457–18462.
- 16 Y. Sakai, Y. Yoshiura and K. Nakazawa, *J. Biosci. Bioeng.*, 2011, **111**, 85–91.
- 17 Y. Guan and W. Kisaalita, *Colloids Surf., B Biointerfaces*, 2011, **84**, 35–43.
- 18 T. C. Chang and P. A. Malian, *J. Manuf. Processes*, 1999, **1**, 1–17.
- 19 Y.-T. Chen, K. Naessens, R. Baets, Y.-S. Liao and A. A. Tseng, *Opt. Rev.*, 2005, **12**, 427–442.
- 20 R. Irawan, S. C. Tjin and C. Y. Fu, *Microwave Opt. Technol. Lett.*, 2005, **45**, 456–460.
- 21 M. C. Liu, D. Ho and Y.-C. Tai, *Sens. Actuators, B*, 2008, **129**, 826–833.
- 22 G. M. Whitesides, *Lab Chip*, 2011, **11**, 191–193.
- 23 Y. Y. Choi, B. G. Chung, D. H. Lee, A. Khademhosseini, J.-H. Kim and S.-H. Lee, *Biomaterials*, 2010, **31**, 4296–4303.
- 24 E. Kang, Y. Y. Choi, Y. Jun, B. G. Chung and S.-H. Lee, *Lab Chip*, 2010, **10**, 2651–2654.
- 25 L. Kang, M. J. Hancock, M. D. Brigham and A. Khademhosseini, *J. Biomed. Mater. Res., Part A*, 2010, **93**, 547–557.
- 26 Y.-S. Hwang, B. G. Chung, D. Ortmann, N. Hattori, H.-C. Moeller and A. Khademhosseini, *Proc. Natl. Acad. Sci. U. S. A.*, 2009, **106**, 16978–16983.
- 27 J. Miranda, M. J. T. Carrondo and P. M. Alves, 3D Cultures: Effect on the Hepatocytes Functionality, in *Cells and Culture*, ed. T. Noll, Springer, Netherlands, 2010, pp. 171–176.
- 28 A. Abbott, *Nature*, 2003, **424**, 870–872.
- 29 Y. Sakai, S. Yoshida, Y. Yoshiura, R. Mori, T. Tamura, K. Yahiro, H. Mori, Y. Kanemura, M. Yamasaki and K. Nakazawa, *J. Biosci. Bioeng.*, 2010, **110**, 223–229.